

## Cross sections and threshold effects for electron-impact excitation of the $(2s^2)^1S$ and $(2s2p)^3P$ states of helium\*

David Spence

Argonne National Laboratory, Argonne, Illinois 60439

(Received 14 July 1975)

The energy and intensity of scattered electrons resulting from excitation of the  $(2s^2)^1S$  and  $(2s2p)^3P$  autoionizing states of helium have been measured as a function of incident electron energy. For incident energies only slightly higher than the threshold for  $(2s^2)^1S$  excitation, post-collision interactions between the scattered and ejected electrons cause the slowly moving scattered electron to lose an amount of energy proportional to  $E_{ex}^{-1.25 \pm 0.05}$  (where  $E_{ex}$  is the energy the scattered electron would have had in the absence of a post-collision interaction). This energy dependence compares well with an energy gain of the ejected electron proportional to  $E_{ex}^{-1.2}$ , obtained by previous workers. Measurements of the intensity of scattered electrons show that both  $^1S$  and  $^3P$  total cross sections peak at threshold and have magnitudes about  $(2.0$  and  $4.0) \times 10^{-20}$  cm<sup>2</sup>, respectively, then rise to broad maxima of magnitudes about  $(2.5$  and  $5) \times 10^{-20}$  cm<sup>2</sup> about 4.0 eV above their thresholds. A subsidiary peak at 59.0 eV in the  $^3P$  cross section is attributed to decay of the previously unidentified  $(2s2p^2)^2S$  He<sup>-</sup> state into the  $^3P$  channel. The magnitude, energy, and width of this resonant structure in the  $^3P$  channel agrees with theoretical predictions.

### I. INTRODUCTION

Studies of doubly excited states in helium to date have included electron-impact energy-loss measurements,<sup>1-3</sup> electron-impact threshold measurements,<sup>4-6</sup> high-energy ion-impact measurements,<sup>7</sup> optical-excitation measurements,<sup>8</sup> inelastic decay modes,<sup>9-11</sup> studies of structures in the total ionization-efficiency curve,<sup>12</sup> and photoabsorption measurements.<sup>13</sup> Most of these measurements are concerned mainly with line positions and profiles.

Recent studies of the  $(2s^2)^1S$ ,  $(2s2p)^3P$ ,  $(2p^2)^1D$ , and  $(2s2p)^1P$  autoionizing states of helium have been made near their thresholds for excitation by electron impact. Studies by Hicks *et al.*<sup>9</sup> and Smith *et al.*<sup>10</sup> reveal that features in the spectra of electrons ejected from these states shift to higher energy as the energy of the incident electrons is lowered to within a few eV of the excitation thresholds. This phenomenon has been interpreted<sup>9,10,14</sup> as a "post-collision interaction" (PCI) between the slow scattered electron and the fast ejected electron. An analogous interaction between ejected and scattered particles has previously been observed in the scattering of low-energy helium ions from helium atoms by Barker and Berry.<sup>15</sup> The PCI phenomenon can be briefly described as follows: If the lifetime of the autoionizing state is sufficiently short, then the fast-moving ejected electron can gain energy by Coulomb repulsion from the slow-moving scattered electron. The energy gain of the ejected electron is greatest when the lifetime in the autoionizing state is short so that the scattered electron is still in close proximity to the autoionizing atom, and the excess energy of the incident electron is small (where the excess energy  $E_{ex}$  is de-

defined as the energy that the scattered electron would have had in the absence of a PCI). The gain in energy of the ejected electron should, of course, be counterbalanced by a corresponding loss in energy by the scattered electron. Because of experimental limitations, study of this phenomenon by measurements of the loss of energy of the scattered electron have to date been restricted to electrons whose scattered energy is essentially zero.<sup>9</sup>

In the present experiments we use a modulated potential-well technique<sup>16</sup> to measure the energy loss due to a PCI mechanism for values of scattered-electron energy up to about 7 eV, and thus check the correspondence between the energy loss of the scattered electron and the energy gain of the ejected electron.

To date, no measurements have been reported for total cross sections for electron-impact excitation of doubly excited autoionizing states of He. In this paper we report the first measurements of the total inelastic cross sections for excitation of the  $(2s^2)^1S$  and  $(2s2p)^3P$  autoionizing states from their thresholds to about 7.0 eV above their respective thresholds. We measure these cross sections using a modification of the trapped-electron method<sup>17</sup> which includes modulation of the trapping potential well, a technique first introduced by Knoop and Brongersma.<sup>16</sup>

### II. THE APPARATUS AND MODES OF OPERATION

The apparatus used for the present experiments is shown schematically in Fig. 1, together with a sketch of the electric potential along the axis of the electron beam. Electrons are emitted from a thorium-coated iridium filament F, and a monoener-

getic beam is selected by a trochoidal monochromator<sup>18</sup> (TM). The monoenergetic electron beam is confined by a magnetic field  $B$  and is accelerated through a potential  $V_a$  into the gas-filled collision chamber  $C$ , where a potential well of depth  $W$  is applied by a cylindrical electrode  $M$ . The energy of the electrons in the collision chamber is thus  $e(V_a+W)$ . Electrons which lose an amount of energy between  $eV_a$  and  $e(V_a+W)$  in an inelastic collision with the target gas in the chamber remain trapped in the potential well, where they migrate through  $B$  by multiple elastic collisions with the gas and are collected at  $M$ .

For incident-electron energies  $e(V_a+W)$  sufficient to excite several states located at energies  $E_1, E_2, E_3$ , etc., the energies of inelastically scattered electrons are  $e(V_a+W) - E_1, e(V_a+W) - E_2, \dots$ , and they effectively reside in different energy "strata" in the potential well, as shown in Fig. 1. All of these inelastically scattered electrons are eventually collected at  $M$ . However, by modulating  $W$  by a small amount  $\Delta W$  at electrode  $ME$  and by measuring the ac component of the collected current at  $M$  with a lock-in amplifier, only electrons whose final energy is equal to  $eW$  (within

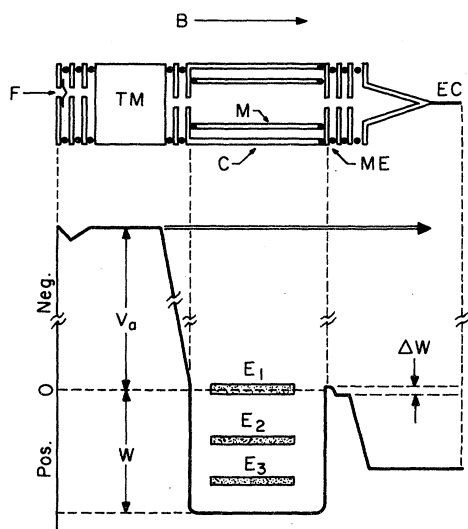


FIG. 1. Schematic diagram of the apparatus and the potential distribution along the axis of the electron beam. The incident-electron energy in the collision chamber is  $e(V_a+W)$ , and those electrons which lose an amount of energy between  $eV_a$  and  $e(V_a+W)$  in an inelastic collision remain trapped in the potential well  $W$  and are collected at  $M$ . By modulating the well by an amount  $\Delta W$ , only electrons whose scattered energy is equal to  $eW$  are detected by a synchronous detector.

$\Delta W$ ) are detected. This modulation technique, first introduced by Knoop and Brongersma,<sup>16</sup> differs from the usual trapped-electron technique<sup>17</sup> in that electrons whose final energy is less than  $eW$  are not detected.

By setting  $eV_a = E_1$  (or  $E_2, E_3$ , etc.), and by increasing  $W$  from zero to a positive value, a signal proportional to the excitation function of the state  $E_1$  (or  $E_2, E_3$ , etc.) is detected at  $M$ . Though this method has been used by some workers to obtain electron-impact excitation functions,<sup>16</sup> there are instrumental effects introduced as  $W$  is increased which render excitation functions obtained by this mode of operation suspect for large values of  $W$ .<sup>19</sup>

In the present experiments, we use an alternative mode of operation which allows measurement of inelastic peak areas rather than peak heights,<sup>19</sup> providing compensation for these instrumental effects; we vary in incident-electron energy by sweeping  $V_a$  rather than by sweeping  $W$ . Using a fixed value of  $W$ , and  $e(V_a+W) < E_1$ , then by increasing  $V_a$ , a signal corresponding to excitation of different states with threshold energies  $E_n$  ( $n = 1, 2, 3, \dots$ ) is obtained whenever  $V_a = E_n$ . The magnitude of this signal is proportional to the inelastic cross section for excitation of the  $E_n$  state at an energy  $eW$  above its respective threshold; i.e., the energy of the detected electrons is always  $eW$ . Above the ionization threshold, any negative-ion resonance features in the ionization continuum will occur when  $e(V_a+W) = E_{\text{resonance}}$ , i.e., whenever  $eV_a = E_{\text{resonance}} - eW$ . Thus, for greater initial values of  $W$ , resonance features in the ionization continuum will occur at lower values of  $V_a$ , in contrast to discrete inelastic features which occur at a value of  $V_a$  independent of  $W$ . These effects are illustrated with reference to Fig. 2, which exhibits the following features:

(a) The circled inset shows a spectrum of singly excited states in helium. Peaks occur in this spectrum whenever  $eV_a$  is equal to the excitation energy of the indicated states as described above.

(b) The two longer traces show spectra corresponding to excitation of doubly excited states. In these spectra the state labeled  $(2s^2)^1S$  does not occur at a value of  $V_a$  independent of  $W$ . This is due to a post-collision interaction which will be described in detail in Sec. III.

(c) The (negative-ion) resonance features,  $(2s^22p)^2P$  and  $(2s2p^2)^2D$ , occur at lower values of  $V_a$  for larger values of  $W$ .

In Fig. 2 the spectrum of singly excited states is obtained by a single energy scan with a time constant of 10 msec/point. The doubly excited spectra are obtained by addition of successive energy scans in a multichannel analyzer, and correspond to a data-acquisition time of about 2 h.

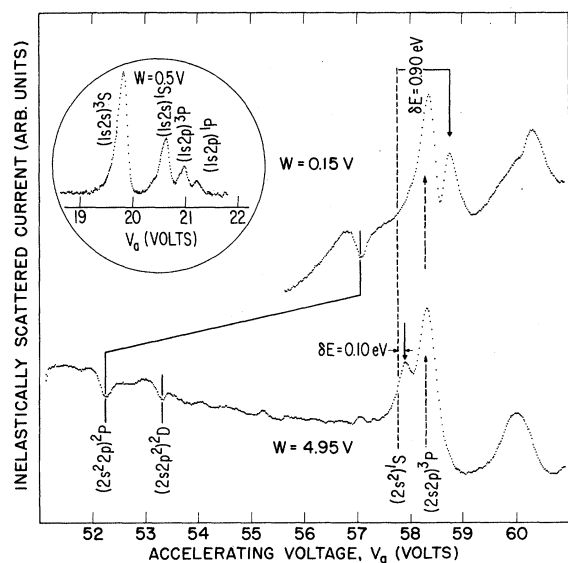


FIG. 2. Spectra of elastically scattered electrons from single and doubly excited states of H for different values of  $W$  (scattered energy  $=eW$ ) as a function of incident energy  $e(V_a + W)$ . Inelastic features occur when  $V_a = E_n$  (where the  $E_n$  are inelastic thresholds), and resonance features occur when the incident energy is equal to a resonance energy, i.e., when  $eV_a = E_{\text{resonance}} - eW$ . Thus at greater values of  $W$  resonant features in the background caused by the ionization continuum appear more to the left in this figure. Note the apparent shift in the  $(2s^2)^1S$  threshold caused by a "post-collision interaction" mechanism.

Because the cross sections for excitation of doubly excited states in helium are quite small, it is desirable to operate with the highest possible target-gas pressure and electron beam currents consistent with the requirement that signal amplitudes are linearly dependent on these parameters. Plots of signal dependence on these parameters are shown over two decades of gas pressure and beam intensity in Figs. 3 and 4, respectively.

In Sec. IV, we determine the cross section for  $(2s^2)^1S$  and  $(2s2p)^3P$  excitation by comparison with the known  $(1s2s)^3S$  cross section 0.5 eV above its threshold. For this reason, we have determined that the ratio of the signals He  $(1s2s)^3S$ /He  $(2s2p)^3P$  is independent of the magnetic field  $B$ , modulation frequency, and modulation voltage  $\Delta W$  for several values of  $W$ . One set of these measurements is shown in Fig. 5. For all measurements described in this paper, we use values of the above parameters indicated by arrows in Figs. 3, 4, and 5.

In the present apparatus, the collection electrode  $M$  is 55 mm long with an inside diameter of 4 mm. Data have been taken with exit holes of the collision chamber (modulating electrode ME) of 4- and 1-mm diam, with no apparent difference in the

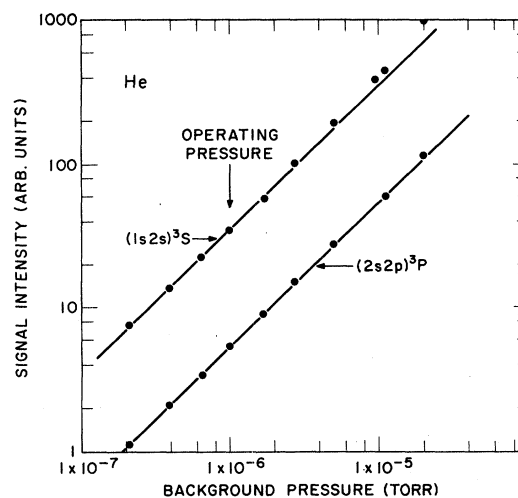


FIG. 3. Plot of the intensity of the He  $(1s2s)^3S$  and  $(2s2p)^3P$  signals as a function of incident electron beam current. The straight lines have slope 1.

ratios of the signals  $(1s2s)^3S/(2s2p)^3P$  for fixed values of  $W$ . However, all data presented in this paper were taken with exit holes of 4-mm diam.

The entire apparatus is constructed from molybdenum, and baked at 400 °C for 24 h before use, giving a base pressure of about  $2 \times 10^{-9}$  Torr.

### III. THRESHOLD EFFECTS

A zero-energy (within  $e\Delta W$ ) scattered-electron spectrum is obtained by setting  $W = 0$  (in which case the incident energy  $E_i = eV_a$ ). Such a spectrum is shown in Fig. 6, together with a threshold-elec-

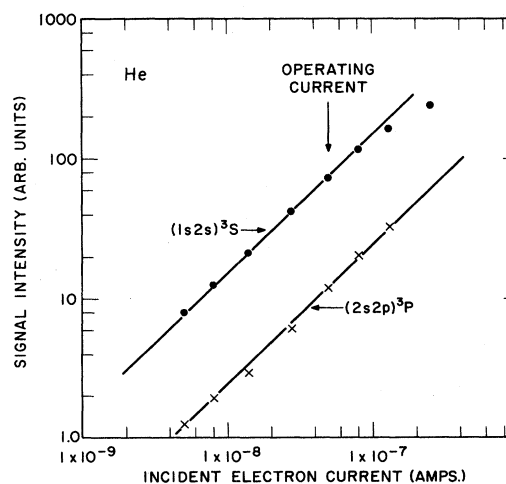


FIG. 4. Plot of the intensity of the He  $(1s2s)^3S$  and  $(2s2p)^3P$  signals as a function of background gas pressure. The straight lines have slope 1. Target-gas pressures are greater by one or two orders of magnitude.

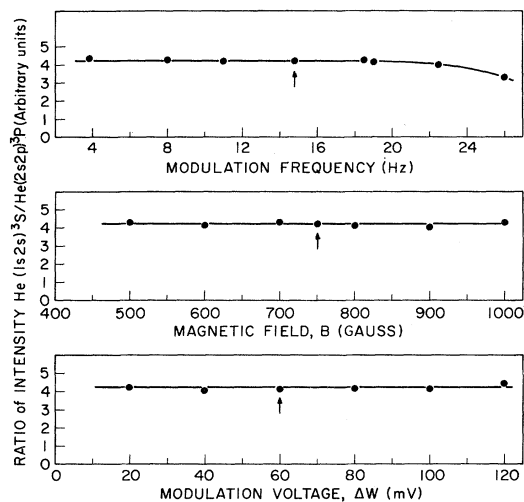


FIG. 5. Plots of the ratios of the He  $(1s2s)^3S$ /He  $(2s2p)^3P$  signal intensities obtained as a function of modulation frequency, magnetic field, and modulation voltage for a value of  $W=0.5$  eV. The vertical arrows indicate the operating conditions used in the present experiments.

tron spectrum (zero-energy spectra) obtained by Hicks *et al.*<sup>9</sup> using a different technique. Though our signal-to-noise ratio is much better than that of Hicks *et al.*,<sup>9</sup> our resolution is considerably worse. A dip in both spectra corresponds to the He<sup>-</sup>  $(2s^22p)^2P$  state located at 57.22 eV,<sup>9</sup> which we use as an energy calibration point. The labeled vertical arrows indicate the energies of the  $(2s^2)^1S$  (57.82 eV) and  $(2s2p)^3P$  (58.35 eV) states obtained from high-energy electron-impact measurements,<sup>9</sup> and from fast helium-ion impact experiments.<sup>7</sup> Both spectra of Fig. 6 show no evidence of any structure at the expected location of the  $(2s^2)^1S$  state (57.82 eV). The absence of a  $(2s^2)^1S$  peak in threshold spectra has previously been noted by Grissom, Compton, and Garrett.<sup>6</sup>

The first inelastic structure in these spectra occur at an energy of 58.35 eV, the location of the  $(2s2p)^3P$  state, a fact also noted by Grissom *et al.*<sup>6</sup> Curiously, the first peak in our spectrum is represented as a doublet in the spectrum of Hicks *et al.*<sup>9</sup> Though we do not resolve this splitting because of insufficient resolution, we suspect this splitting may be due to interference with a negative ion resonance, possibly the  $(2s2p^2)^2D$  state. A second inelastic peak occurs in both spectra at 58.8 eV, though the information contained in Fig. 6 is insufficient to interpret these spectra unambiguously, as no doubly excited state is known to occur at 58.8 eV. However, by taking many spectra similar to those of Figs. 2 and 6 for different values of  $W$  (scattered energy), we observe the 58.8-eV feature

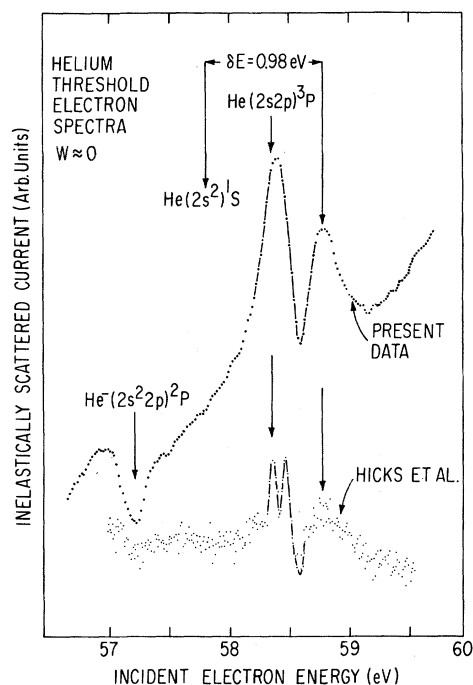


FIG. 6. Threshold electron spectra (i.e., intensities of electrons scattered with essentially zero final energy) in the region of the  $(2s^2)^1S$  and  $(2s2p)^3P$  autoionizing states. The upper curve represents the present data and the lower curve was obtained by Hicks *et al.* (Ref. 9) using a different technique. The  $(2s2p)^3P$  state occurs at its expected energy, but the  $(2s^2)^1S$  state is apparently shifted by 0.98 eV owing to exchange of energy from the scattered electron to the ejected electron by the post-collision interaction mechanism.

of Fig. 2 shifts to lower values of  $V_a$  (i.e., lower apparent threshold) as  $W$  increases. This shifting peak coincides with the  $(2s2p)^3P$  peak when the scattered energy is between 1.0 and 1.5 eV. The lower trace of Fig. 2 shows that for scattered energies of about 5 eV, the shifting feature is almost coincident with the expected location of the  $(2s^2)^1S$  state (57.82 eV) observed from high-energy collision experiments.<sup>7,9</sup> This allows identification of the 58.8-eV feature in the zero-energy spectra in Fig. 6 as being the  $(2s^2)^1S$  state.

A plot of the apparent threshold of the  $(2s^2)^1S$  state as a function of excess energy  $E_{ex}^{-0.5}$  ( $E_{ex} = \delta E + eW$ , the energy the scattered electron would have had in the absence of PCI), is shown in Fig. 7 and illustrates the apparent crossover of these two states as measured from scattered-electron spectra. Also shown in Fig. 7 are the apparent thresholds for  $(2s^2)^1S$  and  $(2s2p)^3P$  excitation measured by Hicks *et al.*<sup>9</sup> from *ejected* spectra; good agreement is shown between the two types of measurements.

Having clearly identified the  $(2s^2)^1S$  state in the zero-energy spectra of Fig. 2, we conclude that for incident-electron energies less than about 1.0 eV above the true threshold for  $(2s^2)^1S$  excitation, the incident electron never emerges from the intermediate complex, though it has sufficient energy to excite this state. Read<sup>20</sup> has suggested that for incident energies close to the  $(2s^2)^1S$  threshold, the ejected electron may gain an amount of energy greater than the excess energy of the incident electron. In such a case, the "scattered" electron will become bound to the residual positive ion core in a highly excited orbital. Smith *et al.*<sup>10</sup> and Heideman *et al.*<sup>11,21</sup> have observed structures in the excitation functions of high- $n$  states corresponding to decay of the  $(2s^2)^1S$  state into these highly excited neutral states, thus lending support to the suggestion of Read.<sup>20</sup>

From measurements of electrons ejected from autoionization of the  $(2s^2)^1S$  state, Smith *et al.*<sup>10</sup> and Read<sup>22</sup> have determined the energy gain of the ejected electron due to PCI to be proportional to  $E_{ex}^{-1.2}$ . In Fig. 8 we have made a log-log plot of  $\delta E$ , the energy lost by the scattered electron, vs the excess energy  $E_{ex}$ . The slope of this plot is  $-1.25$

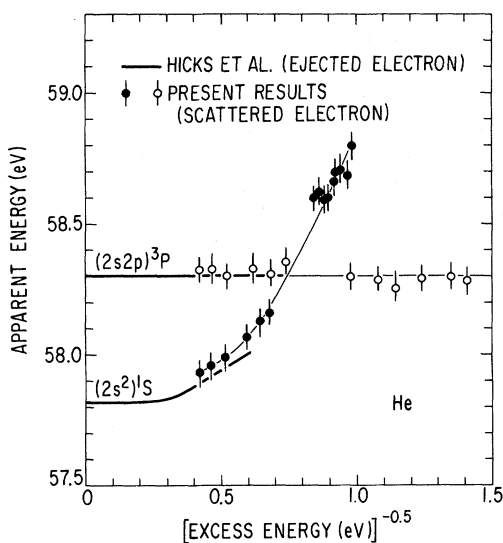


FIG. 7. Plot of the apparent thresholds for  $(2s^2)^1S$  and  $(2s2p)^3P$  excitation as a function of  $E_{ex}^{-0.5}$  obtained from scattered-electron measurements (circles—present data) and ejected-electron measurements [thick solid lines—Hicks *et al.* (Ref. 9)]. The excess energy of the incident electron is defined as the energy the scattered electrons would have had in the absence of a post-collision interaction (i.e.,  $\delta E + eW$  in our experiments). Owing to the crossing of the two inelastic peaks for  $E_{ex} = 1.5$  eV, data points cannot be accurately obtained in this region from scattered-electron measurements.

$\pm 0.05$ , clearly demonstrating the equivalence of the energy lost by the scattered electron with that gained by the ejected electron.

Though the simple PCI model of Barker and Berry<sup>15</sup> predicts an energy exchange proportional to  $E_{ex}^{-0.5}$ , Read<sup>23</sup> has pointed out that the apparent large discrepancy with the value  $E_{ex}^{-1.2}$  for the  $^1S$  state may not be significant because of complications to this simple model from the nearby location of several resonances and the near degeneracy of the  $^1S$  and  $^3P$  states for some values of  $E_{ex}$ . The simple PCI dependence of  $E_{ex}^{-0.5}$  may be expected to be more applicable to the  $(2p^2)^1D$  and  $(2s2p)^1P$  states which occur at higher energy and where the abovementioned complications do not arise. Though we also observe a shift in these higher-energy states, our resolution is insufficient to separate the two states to permit meaningful measurements.

The simple PCI model has recently been extended by King *et al.*<sup>24</sup> to include a semiquantitative explanation of spectral features in high- $n$  excitation functions caused by decay of autoionizing states. This extension of the PCI theory utilizes a "sudden-approximation" model, which describes features in high- $n$  excitation functions as being due to a "shakedown" process, analogous to the "shakeup" or "shakeoff" events well known in Auger-electron spectra.

One should note that not only have shifting thresholds been responsible for inaccurately applied energy scales by many workers, as pointed out by Hicks *et al.*,<sup>9</sup> but also, because of the interchange of location of some of these states as a function of excess energy, wrong state assignments have been made in several published electron spectra.<sup>4-6</sup>

#### IV. CROSS SECTIONS

In the present experiments, total cross sections for excitation of the He  $(2s^2)^1S$  and  $(2s2p)^3P$  states are determined by comparison of the areas of the  $^1S$  and  $^3P$  peaks (obtained from spectra similar to Fig. 2 at different values of  $W$ ) with the area of the  $(1s2s)^3S$  peak obtained at a fixed value of  $W = 0.5$ . The  $(1s2s)^3S$  excitation cross section has been measured absolutely by several workers, and is known to peak 0.5 eV above its threshold.<sup>25</sup> Values of the  $(1s2s)^3S$  cross section at this peak include (in units of  $10^{-18}$  cm<sup>2</sup>)  $2.6 \pm 0.4$  by Fleming and Higginson,<sup>26</sup>  $3.0 \pm 0.7$  by Holt and Krotkov,<sup>27</sup>  $4.0 \pm 1.3$  by Borst,<sup>28</sup>  $4.0 \pm 1.2$  by Schulz and Fox,<sup>29</sup> and 5.0 by Maier-Leibnitz.<sup>30</sup> The most reliable theoretical values for the  $2^3S$  cross section are the recent calculations by Oberoi and Nesbet<sup>31</sup> and by Berrington and Burke.<sup>32</sup> Both of these calculations, though using different theoretical approaches, yield a value of

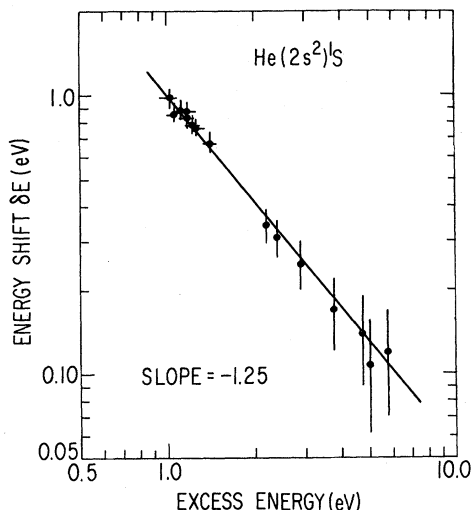


FIG. 8. Log-log plot of the energy shift of the  $(2s^2)^1S$  state as a function of excess energy  $E_{ex}$  obtained from measurements of the scattered-electron energy. The slope,  $-1.25$ , compares with the value  $-1.2$  obtained by Smith *et al.* (Ref. 10) from ejected-electron spectra.

$5.6 \times 10^{-18} \text{ cm}^2$  for the  $2^3S$  cross section 0.5 eV above its threshold. The magnitude of the calculated  $2^3S$  cross section, however, is quite sensitive to the width of the  $\text{He}^- (1s2s^2)^2S$  resonance at 19.35 eV, for which both calculations use the theoretical value of 15 meV.<sup>32,33</sup> Though the calculated width is in agreement with some published measurements,<sup>34,35</sup> it is consistent with others<sup>36,37</sup> which have yielded widths of about 8 or 9 meV. Reduction of the width of the  $(1s2s^2)^2S \text{ He}^-$  state from 15 to 8 meV would reduce the magnitude of the calculated  $(1s2s)^3S$  state to the order of  $4.0 \times 10^{-18} \text{ cm}^2$  at the peak 0.5 eV above threshold.<sup>38</sup> For these reasons, we have chosen the value  $4.0 \times 10^{-18} \text{ cm}^2$  for the  $(1s2s)^3S$  peak as our normalization point. If a different value of the  $2^3S$  cross section is accepted in the future, then the present total excitation cross sections for the  $^1S$  and  $^3P$  doubly excited states will need to be suitably renormalized.

Total electron-impact excitation cross sections of the  $^1S$  and  $^3P$  doubly excited states obtained in the present experiments are plotted as a function of incident energy in Fig. 9. We believe these cross sections to be accurate to within 25% relative to our normalization to the  $2^3S$  cross section, with a reproducibility within 10%. Though the true threshold for the  $(2s^2)^1S$  cross section is located at 57.82 eV, our measurements indicate an apparent threshold at 58.8 eV. Note that these measurements do *not* imply that the  $^1S$  cross section is zero between 57.82 and 58.8 eV. Because we observe scattered electrons only, we cannot measure the  $^1S$  cross section in this energy range. Most of the

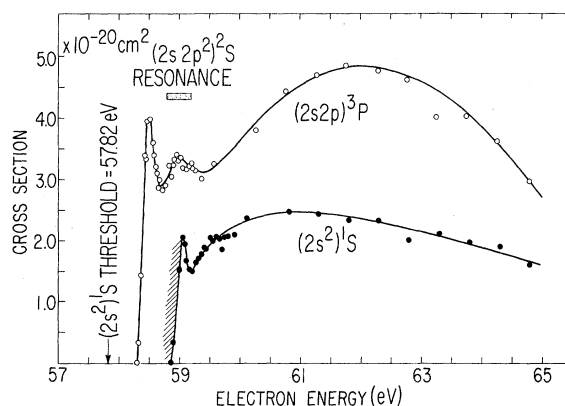


FIG. 9. Total cross sections for electron-impact excitation of the  $(2s^2)^1S$  and  $(2s2p)^3P$  states of He. The crosshatch below the apparent  $(2s^2)^1S$  threshold indicates that we cannot measure this cross section below 58.8 eV from measurements of the scattered electron (as the incident electron never emerges from the intermediate complex), and *not* that the  $(2s^2)^1S$  excitation cross section is zero between 57.82 and 58.8 eV. The sharp rise at threshold of both cross sections is probably due to the  $(2s^22p)^2P$  and  $(2s2p^2)^2D \text{ He}^-$  states which occur just below the inelastic thresholds. The "hump" at 59.0 eV in the  $(2s2p)^3P$  state is interpreted as decay of the broad  $(2s2p^2)^2S$  resonance into the  $^3P$  channel.

incident electrons which have kinetic energies between 57.82 and 58.8 eV and excite the  $^1S$  state will be captured into a highly excited bound orbital, according to the post-collision interaction mechanism. The  $^3P$  cross section (to which the PCI mechanism does not apply because of its long lifetime against autoionization) rises sharply at its expected threshold. The rapid initial rise in both the  $^1S$  and  $^3P$  thresholds is no doubt related to the  $(2s^22p)^2P$  and  $(2s2p^2)^2D \text{ He}^-$  states which lie slightly below the respective inelastic thresholds. The domination of the inelastic cross sections near their thresholds by resonant states at slightly lower energy is well known in the case of singly excited states.<sup>31,32</sup>

Both cross sections in Fig. 9 show the same general shape of a rapid rise followed by a dip, then a slow rise peaking about 4 eV above the respective true thresholds. However, the  $^3P$  cross section exhibits an additional "bump" with a width of about 0.4 eV centered at an incident energy of 59.0 eV. Fano and Cooper<sup>39</sup> have argued that the  $\text{He}^- (2s2p^2)^2S$  state will be located in this energy region, and we attribute the 59.0-eV structure in the  $^3P$  cross section to decay of this  $(2s2p^2)^2S \text{ He}^-$  state into the  $^3P$  inelastic channel.

Theoretical models currently used for calculation of inelastic cross sections are difficult to apply to doubly excited states because of their coupling to the ionization continuum and because of their large polarizability. Ideally, all open chan-

nels must be taken into account in any close-coupling calculation. Despite these difficulties, a close-coupling calculation for electron-impact excitation of the  $(2s2p)^3P$  state has been made by Ormonde *et al.*<sup>40</sup> using a limited number of target eigenstates. These calculations yield the energy of the  $\text{He}^- (2s2p^2)^2S$  state to be 59.4 eV with a width of about 0.30 eV, which decays predominantly into the  $(2s2p)^3P$  channel. Because of the limited number of target eigenstates in their calculation, Ormonde *et al.*<sup>40</sup> find the  $(2s2p)^3P$  excitation cross section to be essentially a single "bump" of magnitude  $\approx 4 \times 10^{-21}$  cm<sup>2</sup> centered at 59.4 eV and with a width of about 0.3 eV, due almost entirely to decay from the  $\text{He}^- ^2S$  state. The calculated magnitude of this bump is in excellent agreement with the bump we observe in the  $^3P$  cross section at 59.0 eV, which has magnitude of about  $4$  or  $5 \times 10^{-21}$  cm<sup>2</sup>, but obviously the theory fails to predict the cross section over an extended energy region.

Support for our value of  $\text{He}^- ^2S$  energy location (59.0 eV) is offered by the measurements of the ionization efficiency of He by Quemener *et al.*<sup>12</sup> Their data show an unexplained bump in the ionization efficiency curve centered at 59.0 eV. The structure observed by Grissom *et al.*<sup>6</sup> at 59.47 eV

in a threshold-electron measurement (and offered by Ormonde *et al.*<sup>40</sup> as evidence of the  $^2S$  state at 59.4 eV) is in reality simply the "valley" between the shifted  $(2s^2)^1S$  peak and the higher-lying  $(2p^2)^1D$  doubly excited state. The discrepancy between the theoretical and experimental energy of the  $(2s2p^2)^2S$   $\text{He}^-$  state is probably not serious; Ormonde<sup>41</sup> has pointed out that by increasing the polarizability of the  $^3P$  state slightly, the calculated  $\text{He}^- (2s2p^2)^2S$  energy is expected to shift to a lower value.

At the present time, the apparent large discrepancy between the experimental and theoretical  $^3P$  cross section (with the exception of the 59.0-eV bump) should likewise not be considered too serious in view of the limited number of initial target eigenstates included in the calculation of Ormonde *et al.*<sup>40</sup> inclusion of a large number of states in the calculation will increase the calculated cross sections accordingly.<sup>41</sup>

#### ACKNOWLEDGMENTS

I wish to express my appreciation to Dr. F. H. Read, Dr. S. Ormonde, Prof. P. G. Burke, and Prof. H. S. Taylor for enlightening discussions, and to Prof. P. D. Burrow for his comments on the manuscript.

\*Work performed under the auspices of the U. S. Energy Research and Development Administration.

<sup>1</sup>R. Whiddington and H. Priestly, Proc. R. Soc. A **145**, 462 (1934).

<sup>2</sup>S. M. Silverman and E. N. Lassette, J. Chem. Phys. **40**, 1265 (1964).

<sup>3</sup>J. A. Simpson, G. E. Chamberlain, and S. R. Mielczarek, Phys. Rev. **139**, A1039 (1965).

<sup>4</sup>P. D. Burrow and G. J. Schulz, Phys. Rev. Lett. **22**, 1271 (1969).

<sup>5</sup>P. D. Burrow, Phys. Rev. A **2**, 1774 (1970).

<sup>6</sup>J. T. Grissom, R. N. Compton, and W. R. Garrett, Phys. Lett. **30A**, 117 (1969).

<sup>7</sup>M. E. Rudd, Phys. Rev. Lett. **13**, 503 (1964).

<sup>8</sup>H. G. M. Heideman, W. Van Dalfsen, and C. Smit, Physica (Utr.) **51**, 215 (1971).

<sup>9</sup>P. J. Hicks, S. C. Cvejanovic, J. Comer, F. H. Read, and J. M. Sharp, Vacuum **24**, 573 (1974).

<sup>10</sup>A. J. Smith, P. J. Hicks, F. H. Read, S. Cvejanovic, G. C. M. King, J. Comer, and J. M. Sharp, J. Phys. B **7**, L496 (1974).

<sup>11</sup>H. G. M. Heideman, G. Nienhuis, and T. van Ittersum, J. Phys. B **7**, L493 (1974).

<sup>12</sup>J. J. Quemener, C. Paquet, and P. Marmet, Phys. Rev. A **4**, 494 (1971).

<sup>13</sup>R. P. Madden and K. Codling, Astrophys. J. **141**, 364 (1965).

<sup>14</sup>F. H. Read, in *The Physics of Electronic and Atomic Collisions, Invited Lectures and Progress Reports of the Eighth International Conference on the Physics of Electronic and Atomic Collisions, Belgrade, Yugoslavia, July 1973*, edited by B. C. Čobić and M. V. Kurepa (Institute of Physics, Belgrade, 1974), pp. 466-476.

<sup>15</sup>R. B. Barker and H. W. Berry, Phys. Rev. **151**, 14 (1966).

<sup>16</sup>F. W. E. Knoop and H. H. Brongersma, Chem. Phys. Letters **5**, 450 (1970).

<sup>17</sup>G. J. Schulz, Phys. Rev. **112**, 150 (1958).

<sup>18</sup>A. Stamatovic and G. J. Schulz, Rev. Sci. Instrum. **41**, 423 (1970).

<sup>19</sup>Strictly speaking, the arguments given above concerning the location of inelastically scattered electrons into different strata are valid only for those electrons scattered in the forward direction. Electrons scattered at angles other than zero, though they may have sufficient energy to escape the well, may be prevented from doing so because their axial velocity vector is insufficient to escape the potential barrier at the end of the tube. These electrons spiral along the magnetic field lines and repeatedly traverse the collision chamber. Successive elastic collisions orient most of these electrons correctly for escape from the well, but a few are always trapped and eventually migrate to the trapped-electron collector M. This phenomenon causes an effective high-energy tail on the discrete strata of electrons sitting in the well. This tail comprises a larger fraction of electrons which have lost a discrete amount of energy at higher values of  $W$ . Thus experiments that measure the peak height of this distribution as a function of incident energy underestimate the cross section at large values of  $W$ .

- This problem, which is intrinsic in the trapped-electron method, may be overcome by measuring the *area* of the scattered-electron effective energy distribution in the well, as we do in our experiments. An additional effect of multiple elastic scattering in the collision chamber is to increase the effective path length with  $W$ , but this effect is negligible in our experiments.
- <sup>20</sup>F. H. Read, Sixth National Conference on Atomic and Molecular Physics, Swansea, England, April 1974 (unpublished).
- <sup>21</sup>H. G. M. Heideman, T. van Ittersum, G. Nienhuis, and M. V. Hol, *J. Phys. B* **8**, L26 (1975).
- <sup>22</sup>F. H. Read, Atomic Physics 4 (Invited Lectures at the Fourth International Conference on Atomic Physics, Heidelberg, 1974) to be published.
- <sup>23</sup>F. H. Read (unpublished).
- <sup>24</sup>G. C. M. King, F. H. Read, and R. C. Bradford, *J. Phys. B* **8**, 2210 (1975).
- <sup>25</sup>F. M. J. Pichanick and J. A. Simpson, *Phys. Rev.* **168**, 64 (1968).
- <sup>26</sup>R. J. Fleming and G. S. Higginson, *Proc. Phys. Soc. Lond.* **84**, 531 (1964).
- <sup>27</sup>H. K. Holt and R. Krotkov, *Phys. Rev.* **144**, 82 (1966).
- <sup>28</sup>W. L. Borst, *Phys. Rev. A* **9**, 1195 (1974).
- <sup>29</sup>G. J. Schulz and R. E. Fox, *Phys. Rev.* **106**, 1179 (1957).
- <sup>30</sup>H. Maier-Leibnitz, *Z. Phys.* **95**, 499 (1936).
- <sup>31</sup>R. S. Oberoi and R. K. Nesbet, *Phys. Rev. A* **8**, 2969 (1973).
- <sup>32</sup>K. A. Berrington and P. G. Burke (unpublished).
- <sup>33</sup>A. L. Sinfailam and R. K. Nesbet, *Phys. Rev. A* **6**, 2118 (1972).
- <sup>34</sup>D. Andrick and H. Ehrhardt, *Z. Phys.* **192**, 99 (1966).
- <sup>35</sup>D. E. Golden, F. D. Schowengerdt, and J. Macek, *J. Phys. B* **7**, 478 (1974).
- <sup>36</sup>J. R. Gibson and K. T. Dolder, *J. Phys. B* **2**, 741 (1969).
- <sup>37</sup>S. Cvejanovic, J. Comer, and F. H. Read, *J. Phys. B* **7**, 468 (1974).
- <sup>38</sup>P. G. Burke (private communication).
- <sup>39</sup>U. Fano and J. W. Cooper, *Phys. Rev.* **138**, A400 (1965).
- <sup>40</sup>S. Ormonde, F. Kets, and H. G. M. Heideman, *Phys. Lett.* **50A**, 147 (1974).
- <sup>41</sup>S. Ormonde (private communication).